Journal of Chromatography A, 1218 (2011) 1891–1898

Contents lists available at ScienceDirect

Journal of Chromatography A

journal homepage: www.elsevier.com/locate/chroma

Characterization of a microelectromechanical systems-based counter-current flame ionization detector

Winfred Kuipers*, Jörg Müller

Hamburg University of Technology, Institute of Microsystems Technology, Eissendorfer Str. 42, 21073, Hamburg, Germany

ARTICLE INFO

Article history:
Received 21 October 2010
Received in revised form 27 January 2011
Accepted 30 January 2011
Available online 2 March 2011

Keywords:
Micro flame ionization detector
MEMS
Microsystems technology
Micro gas chromatography
Total hydrocarbon analysis
FID response mechanism

ABSTRACT

This work is concerned with the influence of different operating parameters on the response of a counter-current micro flame ionization detector (cc-μFID) with low gas consumption for mobile applications. At cc-μFID flow rates (<10 ml/min hydrogen), the response depends mainly on the oxygen flow. At 7.5 ml/min hydrogen flow, highest sensitivity (13.7 mC/gC) is obtained with the smallest flame chamber and nozzle size, moderate sample gas flow (2.0 ml/min), and an oxygen flow above stoichiometry (9.4 ml/min, λ = 2.5). The largest absolute signal is obtained at increased sample gas flow (8.0 ml/min). However, to prevent parting of the micro-flame by the sample gas stream, largest nozzles (smallest outflow velocity) give the best result (4.37 nA). Whereas cc-μFID sensitivity is comparable with conventional FID sensitivity, peak-to-peak noise of 1 pA is relatively large. Therefore, the minimum detectable carbon mass flow of 1.46×10^{-10} gC/s and the minimum detectable methane concentration of 3.43 ppm are larger than typical FID detection limits. μGC–μFID experiments show the difference between premixing the sample with the hydrogen or with the oxygen with respect to sensitivity and response factors. Sensitivity is decreased considerably when the column effluent is added to the oxygen instead of to the hydrogen. For hydrogen premixed samples the response factor to butane can be increased up to 0.81 (methane = 1), whereas for oxygen premixed samples it is maximally 0.31. This smaller sensitivity to oxygen premixed samples and the larger variation of response factors shows the importance of the hydrogen atom during breakdown of organic molecules to single-carbon fragments before ionization.

1. Introduction

The flame ionization detector (FID) is the most popular and widely used detector for the analysis of trace levels of organic compounds. Its success is based on outstanding properties, such as a very low minimum detectable limit (MDL) ($<1 \times 10^{-10}$ gram carbon per second [gC/s]), high sensitivity (0.015 Coulomb per gram carbon [C/gC]) and a broad linear measurement range (10^7) [1]. In addition, the FID is insensitive to modest changes of its operating parameters.

The working principle of the FID is based on the ionization of organic substances in an otherwise non-conducting hydrogen–air diffusion flame [1]. First, hydrocarbon molecules are broken down to single-carbon CH radicals by hydrogen atom induced pyrolysis. Then, these radicals react with oxygen to form CHO^+ ions. It follows that the detector signal is proportional to the number of carbon atoms present in the sample gas. This is also known as the "equal per carbon response" of the FID. Because flame temperature is insufficient for ionization, ionization relies on the large amount of energy released during oxidation of the hydrocarbon radicals. As a result, the FID is insensitive to inorganic compounds and already oxidized substances such as carbon dioxide.

In conventional FIDs, the sample is premixed with the central hydrogen stream of typically 30 ml/min, which is surrounded with a 10-fold amount of air, also to shield the flame from contamination. Both hydrogen and air are supplied from the bottom of the detector vertically upwards.

The research within our group [2–7] and of a few other [8–13] focuses on the miniaturization of the FID to reduce gas consumption for mobile applications. This work reports on the characterization of the latest and most successful version of a MEMS-based FID (μFID), in which the flame burns in the silicon plane of a glass–silicon–glass sandwich. In contrast to previous designs with a single-nozzle micro-burner for premixed hydroxygen flames [4,5], the current μFID is inspired by the work of Hayward and Thurbide [10–13] and consists of an opposed-nozzle micro-burner for extremely stable counter-current diffusion flames (cc-μFID) [6,7]. Hydrogen and oxygen are supplied from opposite directions and react in the vicinity of a so-called stagnation point, where gas flow velocities are small. As a result, also heat loss by forced convection is small and residence times of both fuel

* Corresponding author. Tel.: +49 40 42878 2403; fax: +49 40 42878 2396.
E-mail address: winfred.kuipers@tuhh.de (W. Kuipers).

0021-9673/$ – see front matter © 2011 Elsevier B.V. All rights reserved.
doi:10.1016/j.chroma.2011.01.084

Table 1
Overview of systems and corresponding design parameters. See also Fig. 1c.

System	d (mm)	w_{H_2} (μm)	w_{O_2} (μm)
L1	2	600	600
L2	2	300	600
S1	1	600	600
S2	1	300	600
S3	1	300	300
S4	1	150	300

(complete combustion) and sample (maximum ion yield) are long.

MEMS design and fabrication are described in detail in [7]. It also includes an electrostatic FEM model and FEM simulations of flow and convection, which show the advantages of further downsizing micro-burner dimensions. These results were experimentally confirmed by flame observations, saturation voltages and sensitivities for all systems given in Table 1. This paper is concerned with the influence of operating parameters, such as hydrogen, oxygen and sample gas flow, as well as sample concentration on the characteristics (saturation voltage and sensitivity) of cc-μFIDs of different dimensions (Table 1). If relevant, the results are supported by flame observations. Furthermore, cc-μFID noise is analyzed in view of the MDL. Finally, also the difference with respect to sensitivity and response factors to methane, ethane, propane and butane, between adding the sample to the hydrogen or to the oxygen is determined using a micro-gas chromatograph (μGC).

2. Experimental

2.1. MEMS design and fabrication

The counter-current diffusion flame burns in the silicon plane of an anodically bonded glass–silicon–glass sandwich (Fig. 1a and b). The exhaust openings are small and prevent contamination from the environment. Therefore, there is no need for the excessive airflow, shielding the flame, as in conventional systems and the cc-μFID can be driven with pure oxygen for combustion only. Thermal isolation by low thermal conductive glass minimizes heat loss from the system. Consequently, stable counter-current flames with a reasonable sensitivity of 3.6 mC/gC can be obtained at 5 ml/min hydrogen only [6].

Orthogonal dimensions of the micro-burner, including wafer thickness (500 μm), the nozzle height (100 μm) and the depth of the cavity in the top glass substrate (300 μm), are based on preliminary results [4,5]. The outlet width measures 700 μm. Other in plane dimensions, such as the width of the nozzles w and the distance between the nozzles d (Fig. 1c) vary for the systems examined in this work (Table 1). At moderate gas flows, sensitivity increases with decreasing w and d [7].

Typically, the sample is premixed with the hydrogen (normal FID operation mode). It can also be premixed with the oxygen. Either way, only two gas inlets suffice. The gas inlets, as well as the cavity in the top glass substrate (Fig. 1b) are realized by HF wet etching from both sides of the substrate simultaneously. The structures in the silicon substrate are anisotropically etched by deep reactive ion etching (DRIE).

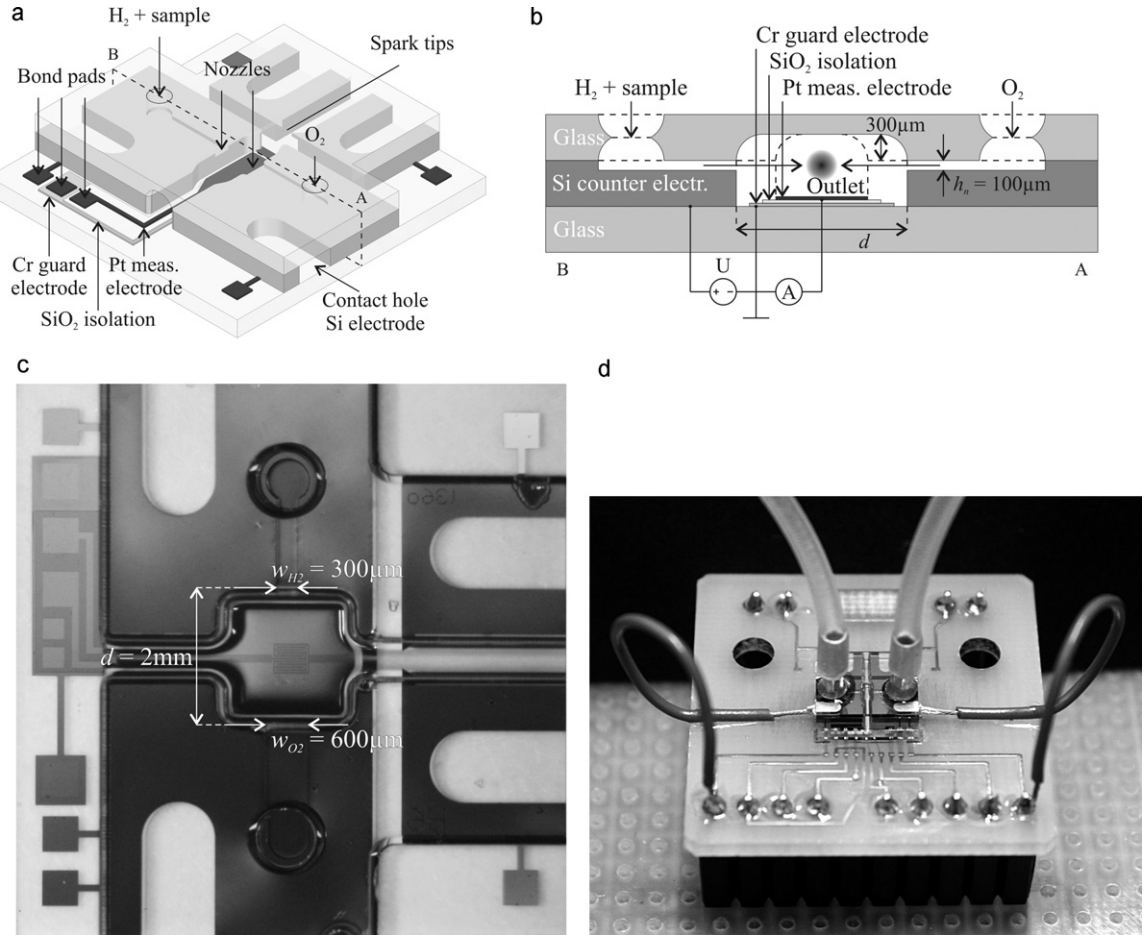

Fig. 1. 3D representation (a), cross-section (b), top view photo (c), and measurement interface (d) of the cc-μFID. The dice measures 8 mm × 8 mm and each substrate is 500 μm thick.

The polarization voltage is applied between the silicon and a sputtered platinum thin film measurement electrode on the bottom glass substrate. At elevated temperatures the borosilicate glass becomes conductive. This is a prerequisite for anodic bonding, but also causes a leakage current during FID operation. This leakage current may be many times larger than the ion current to be measured. Yet, this leakage current can be intercepted by a guard electrode [4]. This guard electrode is realized as a sputtered chromium thin film underneath the measurement electrode and an electrically isolating sputtered silicon oxide layer (Fig. 1b). The platinum measurement electrode is patterned by sputter etching, the chromium and oxide layers by wet chemical etching.

Flames are ignited by a high voltage discharge between two tips in the silicon bulk with 300 μm inter tip distance (Fig. 1a and c). The thin film electrodes are wire bonded to a PCB underneath the cc-μFID (Fig. 1d). The silicon electrode is connected by a wire fixed in a silicon contact hole with conductive silver (Fig. 1d).

2.2. Measurement setup

Fig. 1d shows the fluidic and electrical connections to the cc-μFID. First, the cc-μFID is glued to a small (3.5 cm × 3.5 cm) PCB. Then, aluminum wire bonds are placed from the platinum bond pads on the cc-μFID to copper pads on the PCB. Next, 0.75 mm diameter wire-end sleeves are glued to the cc-μFID gas inlets with a two-component adhesive on an epoxy resin base. Small wires are glued into the silicon contact holes with conductive silver. The opposite wire ends and several multi-pin connectors are soldered to the PCB. The PCB can be plugged onto a larger perfboard, which contains the induction coil circuit for ignition [7] and a triax jack, as well as banana jacks to connect a pA-meter with integrated voltage source (Keithley 487, Cleveland, OH, USA).

Gases are supplied via silicone tubing with an inner diameter of 1 mm (1.8 mm outer diameter), which nicely fits to the 1/16″ Swagelok® tubing of the gas supply system and to the wire-end sleeves on the microsystem. In case of μGC–(μTCD–)μFID, a capillary (75 μm i.d.) is connected to the outlet of the μTCD and together with a second capillary for the hydrogen or oxygen supply glued into a wire-end sleeve, which is then attached to the corresponding wire-end sleeve on the cc-μFID by a short silicone tube.

The hydrogen (5.0) and oxygen (4.8) (both from Air Liquide, Paris, France) flows are controlled by mass flow controllers (MFCs) (Bronkhorst EL-FLOW F201CV, Ruurlo, The Netherlands). Apart from hydrogen and oxygen supply, two different setups can be distinguished. The first setup allows for a continuous flow of sample gas, which is added to the hydrogen. The sample gas consists of a nitrogen-based hydrocarbon containing calibration gas, which can be diluted with pure nitrogen (5.0, Air Liquide, Paris, France). Both gas flows are controlled by MFCs, such that also sample concentration can be adjusted.

The second setup allows for μGC separation of the different constituents of the calibration gas. The column effluent is either added to the hydrogen or to the oxygen. The helium carrier gas flow (6.0, Air Liquide, Paris, France) and the calibration gas flow into the μGC (SLS Microtechnology GCM5000, Hamburg, Germany) are controlled by the input pressure. The micromachined separation column of 270 mm length and 0.3 mm diameter is packed with HayeSep A (Vici, Hayes Seperations Inc., Bandera, Texas, USA).

Photographs of the counter-current diffusive microflames are made with a standard SLR camera connected to a trinocular stereomicroscope above the horizontally aligned cc-μFID. Since the hydrogen flame itself is invisible, the hydrogen gas is bubbled through isopropanol before entering the microsystem to yield a blue colored flame. 20 s exposure time yields photographs with sufficient brightness and contrast. The photographs of blue flames on a black background are edited as greyscale flames on a transparent background.

2.3. Measurement procedures

Unless mentioned otherwise, all measurements were performed with 7.5 ml/min hydrogen, 7.5 ml/min oxygen and a continuous sample gas flow 2.0 ml/min. The sample gas consisted either of the calibration gas (current vs. voltage measurements only), pure nitrogen, or both (sensitivity measurements only). Most experiments were carried out with a calibration gas containing 1% methane in nitrogen (Real Gas, Martinsried, Germany). The calibration gas used for μGC measurements (N21 by Air Liquide, Paris, France) contains 10% methane, 1% ethane, 1% propane and 1% butane in nitrogen. The applied polarization voltage (50, 100 or 150 V) guaranteed ion current saturation for sensitivity measurements.

2.3.1. Current vs. voltage

Typically, at low polarization voltages, the ion current increases linearly with voltage, because recombination is increasingly suppressed. At high voltages, the current saturates smoothly, until all ions reach the electrode at the saturation voltage. Only the saturated ion current is a measure for the organic carbon content in the sample gas and therefore the applied voltage has to be high enough to guarantee saturation. A (linear) increase of the current beyond the saturation voltage implies the presence of a leakage current. In the cc-μFID, the leakage current is suppressed by the guard electrode. The current difference measured between −100 and 100 V, when instead of a hydrocarbon containing calibration gas, pure nitrogen is supplied, is typically less than 100 pA [7]. Subtracting the leakage current (pure nitrogen) from the measured current (calibration gas) yields the true ion current.

Starting at 0 V the polarization voltage was slowly reduced to −100 V first, before it was stepwise increased to 100 V and reduced again to 0 V. The interval from −100 to 100 V was selected for comparison of different settings. Because of charging, the current was allowed to settle for 2 min, before the next voltage step was applied.

2.3.2. Ion current and sensitivity

FID sensitivity s is defined as:

$$s = \frac{I_{\text{ion}}}{\dot{m}_{\text{C}}} \tag{1}$$

where I_{ion} is the ion current in A and $\dot{m}_{\text{C}}$ the carbon mass flow in gC/s. Sensitivity is thereby expressed in C/gC.

To obtain the sensitivity, the ion current was measured at a defined and at zero carbon mass flow (offset correction). The non-zero carbon mass flow was obtained by setting the calibration gas flow to 75% of the total sample gas flow, which was completed with nitrogen. For the linearity measurements, the ion current was measured for four different calibration gas flows (75, 50, 25 and 0% of the total sample gas flow).

After each change of carbon mass flow, the ion current was measured during 5 min, at 5 Hz sampling frequency and 20 ms integration time (line cycle). The average of the final 50 measurements (10 s) was taken as the result.

2.3.3. Noise and MDL

The MDL is defined as the absolute or relative amount of analyte generating a signal, which is twice as large as peak-to-peak noise. Since the FID is an absolute detector, usually the minimum detectable organic carbon mass flow is asked. Sometimes the minimum detectable concentration is useful, e.g. for comparison with relative detectors, such as the TCD. The minimum detectable limit

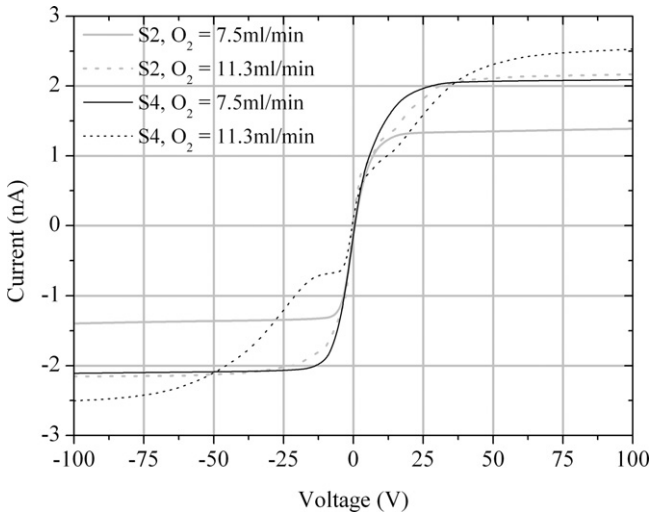

Fig. 2. Current as a function of voltage recorded with systems S2 and S4 at two different oxygen flows.

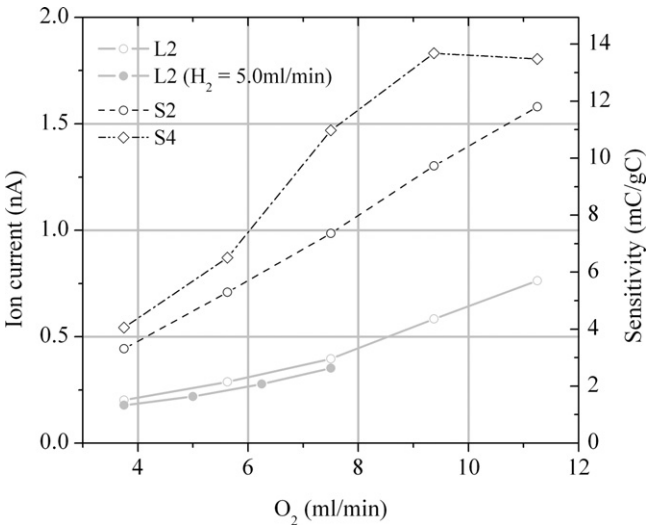

Fig. 3. The influence of the hydrogen and oxygen flow on sensitivity. Unless indicated otherwise, the hydrogen flow is set at 7.5 ml/min.

(in gC/s or ppm) is calculated by dividing two times peak-to-peak noise (in A) by the sensitivity (in C/gC or A/ppm).

Peak-to-peak noise is defined as the difference between the minimum and the maximum value of a 1 s (5 measurements) moving average during the final 60 s of a zero (pure nitrogen) measurement, after long term noise, represented by a 10 s moving average, has been subtracted.

2.3.4. GC–μFID

The cc-μFID was connected to a μGC to determine the difference between hydrogen and oxygen premixed samples in sensitivity and response factors to the four different hydrocarbons contained in N21. In case of 2 ml/min continuous sample supply to the oxygen, the flame would move even more towards the hydrogen nozzle. With the μGC setup the movement was small, since the helium carrier gas flow was set at 1 ml/min only and helium is seven times lighter than nitrogen. Moreover, 2 ml/min nitrogen was continuously added to the hydrogen.

The total injection volume consisted of 8 multiple injections of 1 μl. After a delay of 6 s, the column was heated from 40 to 165 °C in 62.5 s (2 K/s). The sensitivity to a certain hydrocarbon molecule was determined by dividing the corresponding peak area (in C) by its injected carbon mass (in gC).

3. Results and discussion

3.1. Current vs. voltage

3.1.1. The influence of the oxygen flow

Fig. 2 depicts current vs. voltage characteristics recorded with systems S2 and S4 at two different oxygen flows (7.5 and 11.3 ml/min). The saturation current as well as the saturation voltage increase with the oxygen flow (compare solid and dotted lines in Fig. 2). The latter is supposed to increase due to both, the increased saturation current and the increased flow velocity.

There is a remarkable difference between the behaviors of the two systems at large oxygen flow (compare dotted lines in Fig. 2). Although both curves slightly deviate from the typical S-shaped curve at positive voltages, the curve recorded with S4 contains an intermediate plateau at negative voltages. Similar behavior was observed by others. Whereas Desty et al. [14] explained the plateau by positive charge carriers of different mobility, Dewar [15] attributed this behavior to space charge effects. Blades [16] postulated that a complete explanation must also include gas flow.

3.1.2. The influence of the sample gas flow

The sample gas (1% methane in nitrogen) flow was increased in equal steps of 2.0 ml/min up to 8.0 ml/min to determine its influence on ion current saturation. As expected, the saturation current increases with the sample gas or carbon mass flow. So does the saturation voltage.

3.1.3. The influence of the sample concentration

To determine the influence of the sample concentration on ion current saturation, samples of 1 and 10% methane in nitrogen were compared. For a system of type S2, the ion current obtained with 1% methane saturates at +25 V. With 10% methane it saturates at +100 V. Since flow velocities were identical, it follows that the saturation voltage increases with the saturation current.

In general, saturation sets in at smaller negative than positive voltage. Also, in Fig. 2, the intermediate plateau is more pronounced at negative voltage. This asymmetry cannot be explained by the asymmetry of the electrode arrangement alone, but probably exists also because of the different mobilities of positive and negative charges.

3.2. Sensitivity

3.2.1. The influence of the hydrogen and oxygen flow

In Fig. 3 both the influence of the hydrogen and oxygen flow on the cc-μFID sensitivity are shown. Only systems with asymmetric nozzles are considered. The sensitivity of a system of type L2 was determined for hydrogen flows of 5.0 and 7.5 ml/min and different oxygen flows. In this flow range, sensitivity depends more on the oxygen than on the hydrogen flow.

At this point it is useful to introduce the equivalence ratio λ:

$$\lambda = \frac{x_{O_2}/x_{H_2}}{x_{O_2,st.}/x_{H_2,st.}} = 2\left(\frac{x_{O_2}}{x_{H_2}}\right) \quad (2)$$

where x_{O_2} is the mole fraction of oxygen and $x_{O_2,st.}$ the mole fraction of oxygen in a stoichiometric mixture with hydrogen. Accordingly, $\lambda = 1$ corresponds to a stoichiometric mixture and $\lambda > 1$ refers to oxygen rich conditions. It follows from Fig. 3 that sensitivity profits more from an increase of λ by raising the oxygen flow, than from a decrease of λ (towards stoichiometry) by raising the hydrogen flow. Therefore, the remainder of this section deals with the influence of the oxygen flow on sensitivity, rather than with the influence of the hydrogen flow.

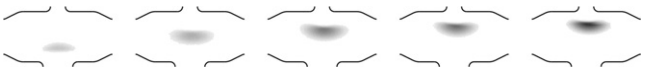

Fig. 4. The influence of the oxygen flow on the brightness of flames in a type S2 system. The flames correspond to the oxygen flows from Fig. 3. Hydrogen (+ sample) is supplied from the top and oxygen from the bottom.

For all, but systems of type S4, sensitivity increases with the oxygen flow at least up to 11.3 ml/min ($\lambda = 3$), which is the maximum oxygen flow examined in this work. Overall maximum sensitivity (13.7 mC/gC) is obtained with S4 at 9.4 ml/min oxygen ($\lambda = 2.5$). For conventional FIDs, air flows as large as $\lambda = 6$ [14] may be needed to obtain a flat, air flow independent response. In general, 10 times as much air as hydrogen is supplied ($\lambda = 4$).

Fig. 4 shows flames of a type S2 system, which correspond to the experiment of increasing oxygen flow (Fig. 3). With increasing oxygen flow, the flames not only move towards the hydrogen nozzle, but also become brighter. This is expected, since for both, chemi-luminescence from excited CH and C_2 radicals (Swan bands in the blue part of the visible spectrum) and chemi-ionization of CH radicals, similar energetic criteria have to be satisfied [17].

Also, the confinement of the flammable mixture, which is related to brightness and sensitivity, increases with the oxygen flow. The latter demonstrates the advantage of small nozzles (S4), which give large outflow velocities and consequently a more confined flammable mixture [7].

3.2.2. The influence of the sample gas flow

One way to improve detector performance is increasing its sensitivity, e.g. by increasing the oxygen flow. Another way to increase the detector signal is by injecting more sample gas. The impact of the sample gas flow on the ion current, as well as the maximum allowed sample gas flow with respect to flame stability was investigated at a constant oxygen flow of 11.3 ml/min and for systems with the smaller nozzle distance of 1 mm (S) only. The results are shown in Fig. 5. The trivial points at the origin were added to the result. For systems S1 and S3 (symmetric nozzles), sensitivity decreases only slightly with increasing sample gas flow up to flame instability beyond 8, respectively 4 ml/min. 4.37 nA (S1 at 8 ml/min sample gas flow) is the largest ion current obtained with a cc-μFID for a methane concentration of 0.75% in nitrogen.

In contrast to symmetric (S1 and S3), the sensitivity of systems with asymmetric nozzles (S2 and S4) decreases with increasing sample gas flow (Fig. 5). In fact, sensitivity collapses, such that for system S2 the ion current at 8 ml/min is even smaller than at 4 ml/min sample gas flow. This is nicely illustrated by the corresponding flame photo at 8 ml/min sample gas flow (Fig. 6). The flame is split in half (dumbbell-shaped flame) by the large gas flow velocity from the hydrogen nozzle. Since heat loss from the flame scales with its surface-to-volume ratio, the flame temperature is decreased. Consequently, also brightness and sensitivity are reduced. A significant decrease in sensitivity and the formation of dumbbell-shaped flames are observed at the same sample gas flow for system S4 as well. Although such dumbbell-shaped flames survive sample gas flows of 12 ml/min or more, the largest ion current for a methane concentration of 0.75% in nitrogen does not exceed 4 nA.

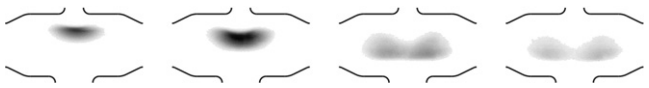

Fig. 6. The influence of the sample gas flow on flames in a type S2 system at 11.3 ml/min oxygen flow. The flames correspond to the sample gas flows from Fig. 5 starting at 2.0 ml/min. Hydrogen (+ sample) is supplied from the top and oxygen from the bottom.

In summary, the largest sensitivity of 13.7 mC/gC is found for a system of type S4 (smallest nozzles) at 2 ml/min sample gas flow and 9.4 ml/min oxygen flow. A type S1 (largest nozzles) system generates the largest ion current (4.37 nA) at 8 ml/min sample gas and 11.3 ml/min oxygen flow. The smaller nozzles of type S4 produce the most confined flammable mixtures at moderate sample gas flows. However, at larger sample gas flows, flames become instable (dumbbell-shaped flames) due to the increased flow velocities. Therefore, for larger sample gas flows, the larger nozzles of type S1 are advantageous.

3.2.3. Linearity

Linearity was determined by diluting three different calibration gases (0.1, 1 and 10% methane in nitrogen) in three steps to pure nitrogen. The sensitivities corresponding to the non-zero measurements of two different systems (type L2 and S2) are plotted in Fig. 7. Evidently, the sensitivity decreases systematically with the carbon mass flow for each calibration gas. It is constant if for each calibration gas one measurement point is considered only. The observed anomaly originates from a systematic error in the carbon mass flow. Indeed, the error of the MFC is specified at 0.8% of set-point plus

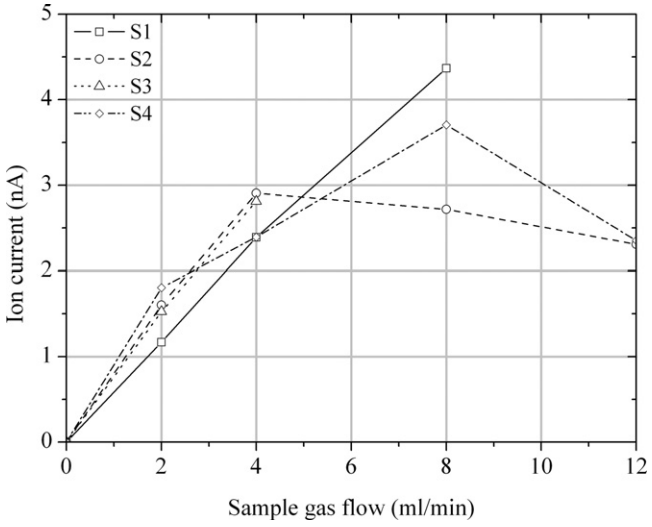

Fig. 5. The influence of the sample gas flow on the ion current at 11.3 ml/min oxygen flow and for small systems only. The slope represents sensitivity.

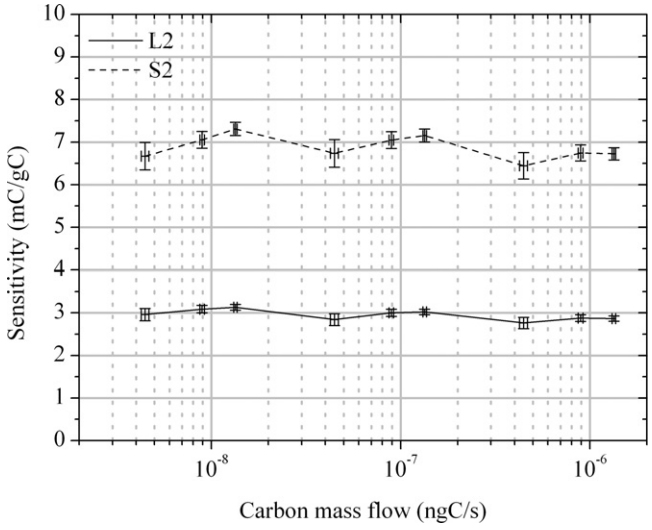

Fig. 7. Sensitivity as a function of carbon mass flow for systems of type L2 and S2. The error bars are based on the specifications of the MFC.

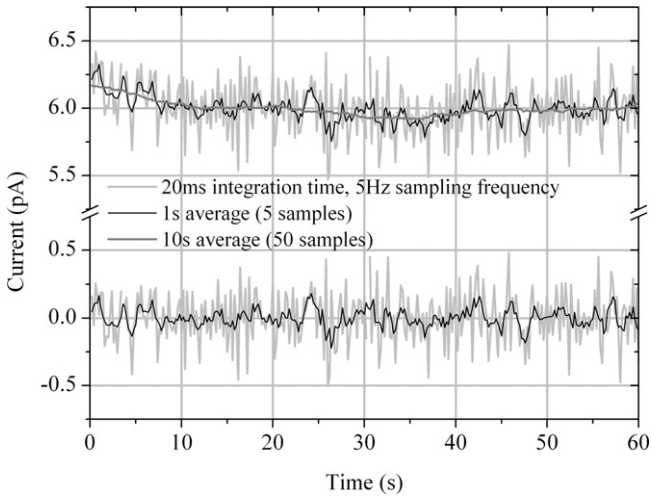

Fig. 8. cc-μFID noise.

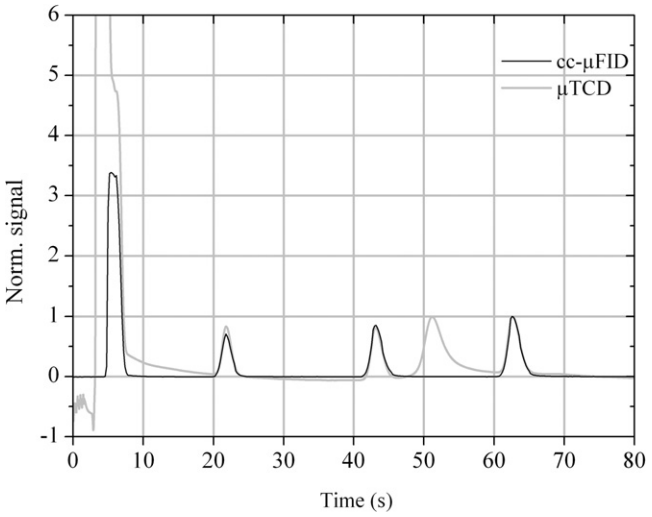

Fig. 9. Chromatograms of the calibration gas N21 (10% methane, 1% ethane, propane, and butane) recorded with the cc-μFID ($H_2 = O_2 = 7.5$ ml/min, $N_2 = 2.0$ ml/min) and the μGC's internal μTCD.

0.2% of full-scale (10 ml/min). Consequently, the error at 0.5, 1.0 and 1.5 ml/min sample gas flow adds up to respectively 4.8, 2.8 and 2.1% of set-point. Referring to the definition of sensitivity (Eq. (1)), the error in sensitivity Δs is given by [18]:

$$\Delta s = \frac{s}{I_{ion}}\Delta I_{ion} + \frac{s}{\dot{m}_C}\Delta \dot{m}_C \quad (3)$$

Neglecting the error of the ion current measurement, equation (3) reduces to:

$$\Delta s = \frac{s}{\dot{m}_C}\Delta \dot{m}_C \quad (4)$$

When Δs is considered in Fig. 7, an almost horizontal line can be drawn through the measurement points. Only a small increase of sensitivity with decreasing carbon mass flow remains. This deviation is presumably caused by organic residuals, which generate an increasing part of the signal, when the carbon mass flow is decreased. It can be concluded that, at least within the examined range of three orders of magnitude, cc-μFID sensitivity varies less than ±5%.

3.3. Noise and MDL

The MDL (either absolute or relative) is limited by the noise. Fig. 8 shows typical cc-μFID noise during a 60 s measurement interval with a polarization voltage of 50 V. The upper light grey line represents the signal as recorded (line cycle integration (20 s) and 5 samples per second). The upper black line is a 1 s (5 samples) moving average of the recorded signal. The lower grey and black lines are obtained when a 10 s moving average (dark grey line) is subtracted from the upper ones. By this, long term noise is removed from the signal, as well as for a declining signal due to organic residuals (first 10 s of Fig. 8) is corrected. Peak-to-peak noise is defined as the difference between maximum and minimum values of the corrected 1 s moving average (lower black line) and measures 0.40 pA in Fig. 8.

Based on all measurements, 1 pA can be assumed as the upper limit for peak-to-peak noise. Then, the minimum detectable carbon mass flow is obtained with largest sensitivity (13.7 mC/gC) and equals 1.46×10^{-10} gC/s. The minimum detectable methane concentration resulting from the largest ion current (4.37 nA) is 3.43 ppm.

There seems to be no correlation between noise and burner geometry, gas flow or offset current. Yet, the noise level appears to increase with the applied polarization voltage. If so, the minimum detectable limit can be improved by reducing the polarization voltage, since saturation is guaranteed below 50 V for small carbon mass flows.

The standard deviation of the noise σ generated by random fluctuations of a volumetric baseline current I_b (fundamental noise) is given by [19]:

$$\sigma = \sqrt{\frac{I_b e}{t}} \quad (5)$$

where e is the elementary charge (1.6×10^{-19} C) and t the integration time. Accordingly, the fundamental noise, corresponding to Fig. 8, is 7 fA, which is considerably smaller than the standard deviation (0.19 pA) of the recorded noise with long term noise correction (lower light grey line in Fig. 8). In the cc-μFID, the baseline is predominantly caused by the leakage current, rather than background ionization in the flame. It is likely that the leakage current flows across the flame chamber surface and Eq. (5) not applies. There may be other than fundamental sources of noise as well. In this context, one should also consider the advice of McWilliam [20], one of the inventors of the FID, against a glass jet. He argued that traces of alkaline ions from the glass would inhibit detector performance.

3.4. μGC–μFID

The difference between addition of the sample to the hydrogen or to the oxygen with respect to sensitivity and response factors to methane, ethane, propane and butane was determined at different hydrogen and oxygen flows for a system of type S1 using a μGC. Typical chromatograms, recorded with the cc-μFID and the μGC's internal μTCD are shown in Fig. 9. It shows some important advantages of the cc-μFID over the μTCD. Firstly, the cc-μFID is insensitive to the injection procedure. Then, the cc-μFID has a constant baseline. Furthermore, the methane peak (6 s) can be measured easily, since the FID is nearly insensitive to nitrogen (4 s).

The usefulness of a μGC–μTCD–μFID system can be illustrated by examination of the unknown peak after 51 s retention time. Since it was not registered by the cc-μFID, the substance must be of inorganic nature. Furthermore, an additional measurement showed that this peak does not scale with the injection volume and therefore must be contained in the carrier gas. It is released in course of the temperature ramp (40–165 °C) of the separation column.

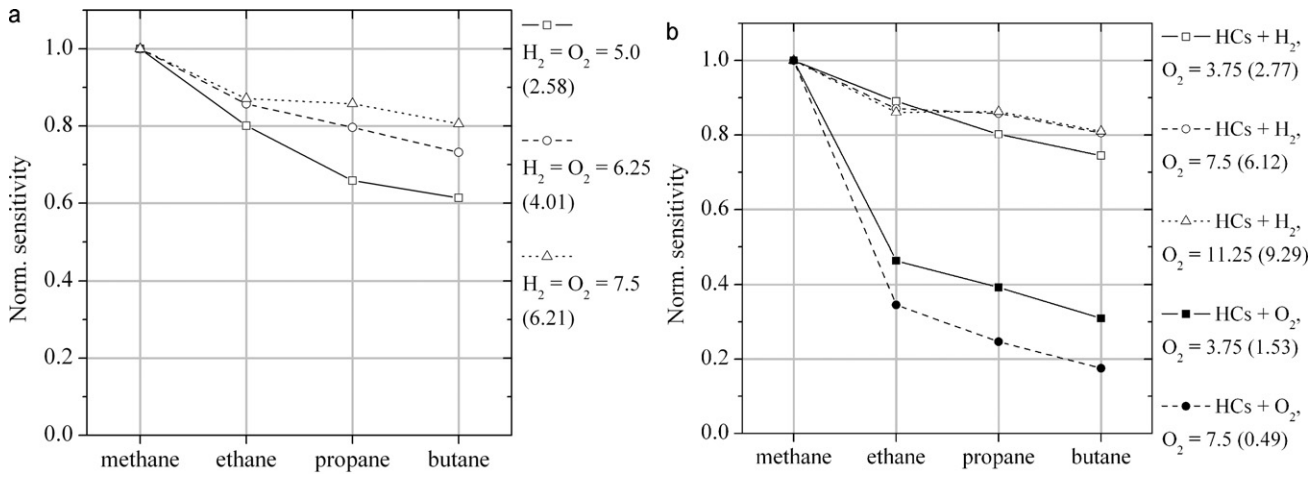

Fig. 10. cc-μFID type S1 response factors to methane (=1), ethane, propane and butane (a) as a function of flame size (equal hydrogen and oxygen flow in ml/min) and (b) as a function of oxygen flow (in ml/min) for hydrogen and oxygen premixed samples. The sensitivity to methane (in mC/gC) is written in between brackets.

From the areas under the peaks the sensitivities to the different hydrocarbon molecules was determined. In Fig. 10 these sensitivities are normalized with respect to methane. The normalized sensitivities can be interpreted as response factors.

Fig. 10a shows the influence of flame size on the response factors for hydrogen premixed samples. With increasing flame size (increasing hydrogen and oxygen flows with constant $\lambda = 2$), the deviance from unity decreases. Whereas, for small flames (5.0 ml/min hydrogen and oxygen flow) the response factor for butane is 0.61, for large flames (7.5 ml/min hydrogen and oxygen flow) it is 0.81. This can be improved only slightly by increasing the oxygen flow up to 11.3 ml/min (Fig. 10b). At stoichiometric oxygen flow (3.8 ml/min), the butane response factor is 0.75.

Fig. 10b also shows the significant influence of adding the column effluent to the oxygen instead of to the hydrogen. Firstly, sensitivity to all four hydrocarbons is reduced considerably. At 7.5 ml/min hydrogen and oxygen flow, the sensitivity to methane is decreased by more than ten times from 6.12 to 0.49 mC/gC. In contrast to the sensitivity to hydrogen premixed samples, the sensitivity to oxygen premixed samples increases (from 0.49 to 1.53 mC/gC), when the oxygen flow is reduced from 7.5 ($\lambda = 2$) to 3.8 ml/min ($\lambda = 1$). The latter can be explained by the fact that with decreasing oxygen flow, an increasing part of the oxygen and consequently of the sample as well, is involved in combustion. Response factors to ethane, propane and butane differ considerably from those to methane. The difference is larger for equal hydrogen and oxygen flow (7.5 ml/min), for which the response factor to butane is only 0.18 (compare 0.81 for hydrogen premixed butane). These results illustrate the importance of the hydrogen atom during breakdown of organic molecules to single-carbon fragments before ionization.

4. Conclusions

In this work the influence of several operating parameters on the response of cc-μFIDs with different dimensions (nozzle size, distance between the nozzles) has been investigated. Within the examined flow range, sensitivity depends more on the oxygen flow than on the hydrogen flow. It is concluded that sensitivity profits more from further increasing λ by increasing the oxygen flow, than from decreasing λ towards stoichiometry by increasing the hydrogen flow.

Highest sensitivity (13.7 mC/gC) is obtained with the smallest system (most confined flammable mixture) by increasing the oxygen flow up to 9.4 ml/min (hydrogen flow = 7.5 ml/min, sample gas (0.75% CH_4 in N_2) flow = 2.0 ml/min). Although the system with the smallest nozzles is most sensitive at moderate sample gas flows, it does not give the largest absolute signal. The latter (4.37 nA) is obtained with the largest nozzles at an increased sample gas (0.75% CH_4 in N_2) flow of 8 ml/min (hydrogen flow = 7.5 ml/min, oxygen flow = 11.3 ml/min). In case of small nozzles, a decrease in sensitivity coincides with the formation of dumbbell-shaped flames at elevated sample gas flow, due to the large flow velocity. Since heat loss from the flame scales with its surface-to-volume ratio, sensitivity and brightness of such a dumbbell-shaped flame are reduced.

Except for the polarization voltage, peak-to-peak noise appears to be independent of operating parameters. At 50 V, it is reasonable to assume 1 pA as the upper limit for peak-to-peak noise. Accordingly, the minimum detectable carbon mass flow equals (2 pA/13.7 mC/gC) = 1.46×10^{-10} gC/s. The minimum detectable methane concentration is (2 pA/4.37 nA × 0.75%) = 3.43 ppm. The MDL can be improved by reducing the polarization voltage, since saturation is guaranteed below 50 V for small carbon mass flows.

μGC measurements confirm the importance of the hydrogen atom during breakdown of organic compounds to single-carbon fragments. When the column effluent is premixed with the oxygen (7.5 ml/min) instead of with the hydrogen (7.5 ml/min), the sensitivity to methane is reduced from 6.12 to 0.49 mC/gC and the response factor of butane relative to methane is reduced from 0.81 to 0.18.

Since the relatively large noise level cannot be explained by fundamental noise only, future work will focus on eliminating non-fundamental noise sources, thereby reducing the MDL.

Acknowledgement

This work has been financially supported by the Deutsche Forschungsgemeinschaft.

References

[1] D.G. McMinn, H.H. Hill, in: H.H. Hill, D.G. McMinn (Eds.), Detectors for Capillary Chromatography, John Wiley & Sons, New York, 1992, 7.
[2] S. Zimmermann, S. Wischhusen, J. Müller, Sens. Actuators, B 63 (2000) 159.
[3] S. Zimmermann, et al., Sens. Actuators, B 83 (2002) 285.
[4] W.J. Kuipers, J. Müller, J. Micromech. Microeng. 18 (2008).
[5] W.J. Kuipers, J. Müller, Talanta 82 (2010) p.1674.
[6] W.J. Kuipers, J. Müller, Proceedings of the 9th Annual IEEE Conference on Sensors (Sensors 2010), Waikoloa, HI, USA, 2010.
[7] W.J. Kuipers, J. Müller, to be published.
[8] C. Deng, et al., J. Chromatogr. Sci. 42 (2005) 355.

[9] C. Washburn, Proceedings of the 4th Annual IEEE Conference on Sensors (Sensors 2005), Irvine, CA, USA, 2005, p. 322.
[10] K.B. Thurbide, B.W. Cooke, W.A. Aue, J. Chromatogr. A 1029 (2004) 193.
[11] K.B. Thurbide, T.C. Hayward, Anal. Chim. Acta 519 (2004) 121.
[12] T.C. Hayward, K.B. Thurbide, Talanta 73 (2007) 583.
[13] T.C. Hayward, K.B. Thurbide, J. Chromatogr. A 1200 (2008) 2.
[14] D.H. Desty, G.J. Geach, A Goldup, Proceedings of the 3rd International Symposium on Gas Chromatography, 1960, Edinburgh, UK, in: R.P.W. Scott (Ed.), Gas Chromatography, Butterworths, London, 1960, p. 46.
[15] R.A. Dewar, J. Chromatogr. 6 (1961) 312.
[16] A.T. Blades, J. Chromatogr. Sci. 11 (1973) 251.
[17] J.F. Griffiths, J.A. Barnard, Flame and Combustion, 3rd ed., Blackie Academic & Professional, London, 1995.
[18] I. de Bruijn, D. van der Meer, B.M. Tel-Berendsen, Fysisch Experimenteren, Universiteit Twente, Enschede, 1999.
[19] W.A. Aue, H. Singh, X.-Y. Sun, J. Chromatogr. A 687 (1994) 283.
[20] I.G. McWilliam, R.A. Dewar, Proceedings of the 2nd International Symposium on Gas Chromatography, Butterworths, London, 1958, p. 142.